Performance comparison of acrylic and thiol-acrylic resins in two-photon polymerization

Lijia Jiang,[1] Wei Xiong,[1,2] Yushen Zhou,[1] Ying Liu,[1] Xi Huang,[1] Dawei Li,[1] Tommaso Baldacchini,[1,3,*] Lan Jiang,[4] and Yongfeng Lu[1,5]

[1]*Department of Electrical Engineering and Computer Engineering, University of Nebraska-Lincoln,Lincoln NE 68588, USA*

[2]*Wuhan National Laboratory for Optoelectronics (WLNO), Huazhong University of Science and Technology, Wuhan, Hubei 430074, China*

[3]*Technology and Applications Center, Newport Corporation, Irvine, CA 92606, USA*

[4]*Laser Micro/Nano-Fabrication Laboratory, School of Mechanical Engineering, Bejing Institute of Technology, Beijing 100081, China*

[5]*ylu2@unl.edu*

[*]*tommaso.baldacchini@newport.com*

Abstract: Microfabrication by two-photon polymerization is investigated using resins based on thiol-ene chemistry. In particular, resins containing different amounts of a tetrafunctional acrylic monomer and a tetrafunctional thiol molecule are used to create complex microstructures. We observe the enhancement of several characteristics of two-photon polymerization when using thiol-acrylic resins. Specifically, microfabrication is carried out using higher writing velocities and it produces stronger polymeric microstructures. Furthermore, the amount of shrinkage typically observed in the production of three-dimensional microstructures is reduced also. By means of microspectrometry, we confirm that the thiol-acrylate mixture in TPP resins promote monomer conversion inducing a higher degree of cross-linked network formation.

OCIS codes: (140.7090) Ultrafast lasers; (160.5470) Polymers; (220.4000) Microstructure fabrication; (140.3390) Laser materials processing.

References and links

1. T. Baldacchini, *Three-Dimensional Microfabrication Using Two-Photon Polymerization: Fundamentals, Technology, and Applications* (Elsevier, 2015).
2. J. Fischer, T. Ergin, and M. Wegener, "Three-dimensional polarization-independent visible-frequency carpet invisibility cloak," Opt. Lett. **36**(11), 2059–2061 (2011).
3. T. Bückmann, M. Thiel, M. Kadic, R. Schittny, and M. Wegener, "An elasto-mechanical unfeelability cloak made of pentamode metamaterials," Nat. Commun. **5**, 4130 (2014).
4. M. K. Driscoll, X. Sun, C. Guven, J. T. Fourkas, and W. Losert, "Cellular contact guidance through dynamic sensing of nanotopography," ACS Nano **8**(4), 3546–3555 (2014).
5. C. N. LaFratta, J. T. Fourkas, T. Baldacchini, and R. A. Farrer, "Multiphoton fabrication," Angew. Chem. Int. Ed. Engl. **46**(33), 6238–6258 (2007).
6. J. T. Fourkas, "Fundamentals of two-photon fabrication" in *Three-Dimensional Microfabrication Using Two-Photon Polymerization: Fundamentals, Technology, and Applications* T. Baldacchini, ed. (Elsevier, 2015).
7. S. Kawata, H.-B. Sun, T. Tanaka, and K. Takada, "Finer features for functional microdevices," Nature **412**(6848), 697–698 (2001).
8. J. Fischer and M. Wegener, "Three-dimensional direct laser writing inspired by stimulated-emission-depletion microscopy," Opt. Mater. Express **21**, 10831–10840 (2013).
9. J. Fischer and M. Wegener, "Three-dimensional optical laser lithography beyond the diffraction limit," Laser Photonics Rev. **7**(1), 22–44 (2013).
10. Z. Gan, Y. Cao, R. A. Evans, and M. Gu, "Three-dimensional deep sub-diffraction optical beam lithography with 9 nm feature size," Nat. Commun. **4**, 2061 (2013).
11. I. Sakellari, E. Kabouraki, D. Gray, V. Purlys, C. Fotakis, A. Pikulin, N. Bityurin, M. Vamvakaki, and M. Farsari, "Diffusion-assisted high-resolution direct femtosecond laser writing," ACS Nano **6**(3), 2302–2311 (2012).
12. W. H. Teh, U. Dürig, U. Drechsler, C. G. Smith, and H.-J. Güntherodt, "Effect of low numerical-aperture femtosecond two-photon absorption on (SU-8) resist for ultrahigh-aspect-ratio microstereolithography," J. Appl. Phys. **97**(5), 054907 (2005).

#263617 Received 22 Apr 2016; accepted 24 May 2016; published 10 Jun 2016

Corrected: 13 June 2016

13. C. A. Coenjarts and C. K. Ober, "Two-photon three-dimensional microfabrication of poly(dimethylsiloxane) elastomers," Chem. Mater. **16**(26), 5556–5558 (2004).
14. J. Torgersen, X.-H. Qin, Z. Li, A. Ovsianikov, R. Liska, and J. Stampfl, "Hydrogels for two-photon polymerization:a toolbox for mimicking the extracellular matrix," Adv. Funct. Mater. **23**(36), 4542–4554 (2013).
15. B. Kaehr, N. Ertas, R. Nielson, R. Allen, R. T. Hill, M. Plenert, and J. B. Shear, "Direct-write fabrication of functional protein matrixes using a low-cost Q-switched laser," Anal. Chem. **78**(9), 3198–3202 (2006).
16. A. Ovsianikov, J. Viertl, B. Chichkov, M. Oubaha, B. MacCraith, I. Sakellari, A. Giakoumaki, D. Gray, M. Vamvakaki, M. Farsari, and C. Fotakis, "Ultra-low shrinkage hybrid photosensitive material for two-photon polymerization microfabrication," ACS Nano **2**(11), 2257–2262 (2008).
17. T. Baldacchini C. N. LaFratta, R. A. farrer, M. C. Teich, B. E. A. Saleh, M. J. Naughton, and J. T. Fourkas, "Acrylic-based resin with favorable properties for three-dimensional two-photon polymerization," J. Appl. Phys. **95**(11), 6072–6076 (2004).
18. L. H. Nguyen, M. Straub, and M. Gu, "Acrylate-based photopolymer for two-photon microfabrication and photonic applications," Adv. Funct. Mater. **15**(2), 209–216 (2005).
19. C. Decker, "Photoinitiated curing of multifunctional monomers," Acta Polym. **45**(5), 333–347 (1994).
20. C. Decker, "Photoinitiated crosslinking polymerization," Prog. Polym. Sci. **21**(4), 593–650 (1996).
21. G. Odian, *Principles of Polymerization* (Wiley-Interscience, 2004).
22. A. R. Kannurpatti, J. W. Anseth, and C. N. Bowman, "A study of the evolution of mechanical properties and structural heterogeneity of polymer networks formed by photopolymerizations of multifunctional (meth)acrylates," Polymer (Guildf.) **39**(12), 2507–2513 (1998).
23. L. Gou, C. N. Coretsopoulos, and A. B. Scranton, "Measurement of the dissolved oxygen concentration in acrylate monomers with a novel photochemical method," J. Polym. Sci. Pol. Chem. **42**(5), 1285–1292 (2004).
24. K. Studer, C. Decker, E. Beck, and R. Schwalm, "Overcoming oxygen inhibition in UV-curing of acrylate coatings by carbon dioxide inerting: part II," Prog. Org. Coat. **48**(1), 101–111 (2003).
25. H. Lu, J. A. Carioscia, J. W. Stansbury, and C. N. Bowman, "Investigations of step-growth thiol-ene polymerizations for novel dental restoratives," Dent. Mater. **21**(12), 1129–1136 (2005).
26. C. E. Hoyle and C. N. Bowman, "Thiol-ene click chemistry," Angew. Chem. Int. Ed. Engl. **49**(9), 1540–1573 (2010).
27. C. E. Hoyle, T. Y. Lee, and T. Roper, "Thiol-enes: chemistry of the past with promise for the future," J. Polym. Sci. Pol. Chem. **42**(21), 5301–5338 (2004).
28. A. S. Quick, J. Fischer, B. Richter, T. Pauloehrl, V. Trouillet, M. Wegener, and C. Barner-Kowollik, "Preparation of reactive three-dimensional microstructures via direct laser writing and thiol-ene chemistry," Macromol. Rapid Commun. **34**(4), 335–340 (2013).
29. R. A. Farrer, C. N. LaFratta, L. Li, J. Praino, M. J. Naughton, B. E. A. Saleh, M. C. Teich, and J. T. Fourkas, "Selective functionalization of 3-D polymer microstructures," J. Am. Chem. Soc. **128**(6), 1796–1797 (2006).
30. Y.-S. Chen, A. Tal, D. B. Torrance, and S. M. Kuebler, "Fabrication and characterization of three-dimensional silver-coated polymeric microstructures," Adv. Funct. Mater. **16**(13), 1739–1744 (2006).
31. X.-H. Qin, J. Torgersen, R. Saf, S. Mühleder, N. Pucher, S. C. Ligon, W. Holnthoner, H. Redl, A. Ovsianikov, J. Stampfl, and R. Liska, "Three-dimensional microfabrication of protein hydrogels via two-photon-excited thiol-vinyl ester photopolymerization," J. Polym, Sci. Polym. Chem. **51**(22), 4799–4810 (2013).
32. B. J. Adzima, C. J. Kloxin, C. A. DeForest, K. S. Anseth, and C. N. Bowman, "3D Photofixation Lithography in Diels-Alder Networks," Macromol. Rapid Commun. **33**(24), 2092–2096 (2012).
33. T. Baldacchini, M. Zimmerley, C.-H. Kuo, E. O. Potma, and R. Zadoyan, "Characterization of microstructures fabricated by two-photon polymerization using coherent anti-stokes Raman scattering microscopy," J. Phys. Chem. B **113**(38), 12663–12668 (2009).
34. L. J. Jiang, Y. S. Zhou, W. Xiong, Y. Gao, X. Huang, L. Jiang, T. Baldacchini, J.-F. Silvain, and Y. F. Lu, "Two-photon polymerization: investigation of chemical and mechanical properties of resins using Raman microspectroscopy," Opt. Lett. **39**(10), 3034–3037 (2014).
35. X. N. He, J. Allen, P. N. Black, T. Baldacchini, X. Huang, H. Huang, L. Jiang, and Y. F. Lu, "Coherent anti-Stokes Raman scattering and spontaneous Raman spectroscopy and microscopy of microalgae with nitrogen depletion," Biomed. Opt. Express **3**(11), 2896–2906 (2012).
36. P. Esfandiari, S. C. Ligon, J. J. Lagref, R. Frantz, Z. Cherkaoui, and R. Liska, "Efficient stabilization of thiol-ene formulations in radicals photopolymerization," J. Polym. Sci. Pol. Chem. **51**(20), 4261–4266 (2013).
37. C. N. LaFratta and L. Li, "Making two-photon polymerization faster," in *Three-Dimensional Microfabrication Using TwoPhoton Polymerization: Fundamentals, Technology, and Applications* T. Baldacchini, ed. (Elsevier, 2015).
38. A. F. Senyurt, H. Wei, C. E. Hoyle, S. G. Piland, and T. E. Gould, "Ternary thiol-ene/acrylate photopolymers: effect of acrylate structure on mechanical properties," Macromolecules **40**(14), 4901–4909 (2007).
39. A. F. Senyurt, C. E. Hoyle, H. Wei, S. G. Piland, and T. E. Gould, "Thermal and mechanical properties of cross-linked photopolymers based on multifunctional thiol-urethane ene monomers," Macromolecules **40**(9), 3174–3182 (2007).
40. A. K. O'Brien, N. B. Cramer, and C. N. Bowman, "Oxygen inhibition in thiol-acrylate photopolymerizations," J. Polym. Sci. Pol. Chem. **44**(6), 2007–2014 (2006).
41. H. B. Sun, T. Suwa, K. Takada, R. P. Zaccaria, M. S. Kim, K. S. Lee, and S. Kawata, "Shape precompensation in two-photon laser nanowriting of photonic lattices," Appl. Phys. Lett. **85**(17), 3708–3710 (2004).
42. M. Deubel, G. von Freymann, M. Wegener, S. Pereira, K. Busch, and C. M. Soukoulis, "Direct laser writing of three-dimensional photonic-crystal templates for telecommunications," Nat. Mater. **3**(7), 444–447 (2004).

#263617 Received 22 Apr 2016; accepted 24 May 2016; published 10 Jun 2016

43. M. P. Patel, M. Braden, and K. W. M. Davy, "Polymerization shrinkage of methacrylate esters," Biomaterials **8**(1), 53–56 (1987).
44. A. Žukauskas, M. Malinauskas, E. Brasselet, and S. Juodkazis, "3D micro-optics via ultrafast laser writing: miniaturization, integration, and multifunctionalities" in *Three-Dimensional Microfabrication Using Two Photon Polymerization: Fundamentals, Technology, and Applications* T. Baldacchini, ed. (Elsevier, 2015).

1. Introduction

Fabrication of three-dimensional microstructures by two-photon polymerization (TPP) has evolved in recent years from a novel technique employed mostly by laser specialists to a useful tool in the hands of scientists and engineers working in a wide range of research fields [1] (the abbreviation TPP is used in this article as a general term for describing photopolymerization induced by n-photon absorption with $n \geq 2$). A perusal of the scientific literature on this topic reveals in fact how extensive the impact of TPP has been in applications that require high precision three-dimensional writing; from the fabrication of optical and mechanical metamaterials to the development of rationally-designed substrates for cell motility studies [2–4].

There are two key reasons that render TPP such an attractive solution for the fabrication of microstructures. The first reason is that TPP is intrinsically a three-dimensional writing technique; it does not require a layer-by-layer approach to create complex objects. The second reason is that TPP can create microstructures with sub-micron feature sizes in a relatively straightforward manner. These characteristics originate from the nonlinear optical nature of light absorption in TPP and from the chemistry of the polymerization that follows [5].

In a typical experiment, near-infrared (NIR) emission is used to excite a photosensitive material (resin) that upon light absorption undergoes a phase change from liquid to solid through a polymerization process. Since the resin is transparent in the NIR region of the spectrum, high numerical aperture (NA) lenses and ultra-short pulsed lasers are employed to increase the probability of a multiphoton absorption event to occur. That is two or more photons are simultaneously absorbed by specialized molecules in the resin (photoinitiators) to create the active species that start polymerization. Under these conditions multiphoton absorption occurs only in the region where light intensity is the highest, thus confining polymerization within the volume of the focused laser beam (voxel). Three-dimensional microstructures are created by precisely overlapping voxels through the scanning of either the laser beam or the sample around predetermined geometries. Successively, the microstructures are revealed by washing away the unsolidified part of the resin using an organic solvent.

The exposure curves of resins employed in TPP are quite nonlinear, thus creating a light intensity threshold below which polymerization does not occur [6]. It is the presence of this intensity threshold that permits the formation of voxels with dimensions that are considerably smaller than the wavelength of light used for fabrication. For example, by adjusting the intensity of the excitation laser barely above the minimum intensity needed to start and sustain TPP, voxels 100 nm wide can be obtained with a typical exposure wavelength of 800 nm [7]. Although the diffraction limit can be broken in TPP using this strategy, writing resolution still suffers from the intrinsic characteristics of the materials employed for polymerization. Because of the so-called "memory effect" of the resin, the minimum achievable distance between two voxels is always two to five times larger than the size of the voxel itself. As a consequence, the highest writing resolution reported so far in TPP is around 200 nm [8].

In recent years, several research groups have developed clever strategies to overcome this limitation, reaching impressive results [9]. In the majority of these techniques, two laser beams with varied spatial and temporal characteristics are used simultaneously to create features with dimensions that are no longer limited by optical diffraction. In all cases, writing resolution was dramatically improved. For example, researchers lately achieved an impressive lateral writing resolution of only 52 nm [10]. TPP writing resolution was also improved using a chemical approach, where a quencher molecule is added to the resin composition [11]. These studies are all very important because they extend the capabilities of TPP well within the realm of nanoscale direct-writing. Furthermore, they investigate the mechanism of light

#263617 Received 22 Apr 2016; accepted 24 May 2016; published 10 Jun 2016

absorption and active species diffusion that take place in TPP thus increasing our comprehension of its mechanism.

The list of negative-tone resins used so far in TPP includes epoxy materials such as SU-8, elastomers such as PDMS, hydrogels, proteins, organic-inorganic hybrids, and multifunctional acrylates [12–17]. Among these, resins based on multifunctional acrylates have received considerable attention [18]. The widespread use of such materials in TPP research is explained by taking into consideration the favorable attributes acrylic monomers and oligomers possess, which render them attractive for microfabrication [19]. Since they are widely used in several industries, acrylic molecules are inexpensive and readily available. They have a relatively stable shelf life, and can be found in a wide assortment of functionalities and sizes. When non polymerized, acrylic-based resins are soluble in common solvents such as ethanol and they are easily processed by spin-coating or drop-casting. Furthermore, acrylates retain high polymerization rates due to their reactivity toward active species such as radicals [20]. To increase the integrity and accuracy of the fabricated three-dimensional microstructure, branched acrylic monomers are typically enlisted in TPP resins. In this way, rigid and insoluble polymer networks are created with a gelation onset that arises at low level of material conversion. Acrylic-based resins are polymerized via a radical chain growth mechanism where several reactions with different rates for initiation, propagation, and termination occur simultaneously [21]. The active species (i.e. radicals) that start the polymerization are created by the photoinitiators following multiphoton absorption. Monomers react only with the propagating reactive center, not with other monomers, and chain addition ceases when the concentration of radicals is depleted by a number of termination reactions.

Despite the numerous advantages acrylic molecules impart to resins used in photopolymerization, they also present some limitations. Specifically, acrylic based resins are notorious in producing inhomogeneous polymer networks and they are sensitive to the presence of dissolved molecular oxygen [22, 23]. The latter interferes with the chain growth mechanism by forming peroxy radicals which do not react rapidly with acrylates. Thus, oxygen has the overall effect of reducing polymerization efficiency by scavenging radicals and effectively terminating them [24]. Several strategies have been employed in the UV curing industry to overcome both of these drawbacks. A common strategy is the addition of thiol molecules to the original acrylic mixture [25]. The relatively weak bond between the sulfur and hydrogen atoms in thiols is capable of transforming the polymerization chemistry, from a pure radical chain growth process to a combination radical chain growth and step growth process, with far-reaching consequences to the chemical and mechanical properties of the ultimate polymer [26]. During photopolymerization, the presence of thiol molecules in the acrylic based resin renders normally unproductive radicals, such peroxide radicals and sterically hindered radicals, “alive” again through a chain transfer mechanism. In this step, hydrogen abstraction occurs between these radicals and thiol molecules, generating thyil radicals which in turn can efficiently add to the carbon-carbon double bonds of acrylates, and in doing so, furthering the degree of polymerization.

Thus, photopolymerization of resin mixtures consisting of acrylates and thiols produce polymer networks from the copolymerization of acrylates with thiols and from the homopolymerization of acrylates [27]. This particular combination of different types of radical polymerization processes generates polymeric structures with highly uniform densities. A clear demonstration of this outcome is the narrow glass-transition region of polymers derived from these resin mixtures, in contrast to the broader one typically obtained from acrylic-based resins only [25]. Moreover, resins with both thiol and acrylic monomers are almost insensitive to the inhibition effect of dissolved oxygen. As a consequence, polymerization rates of acrylic-based resins are accelerated by the addition of thiols with the overall effect of generating polymers with sufficient cure rates, even when the photoinitiator concentration is greatly reduced.

The superior performance of the process and products involved in the photopolymerization of thiol-acrylic resins (and of general thiol-ene resins), have made these

#263617 Received 22 Apr 2016; accepted 24 May 2016; published 10 Jun 2016

materials the center of many research studies with practicality in areas as diverse as optics, microfluidics, and lithography [26]. The TPP community has also taken notice of the improvements brought upon by the use of thiols molecules within resin photopolymerization. In one report, the authors built photonic crystals out of a resin consisting of a multifunctional allylether and a multifunctional thiol [28]. By confirming the presence of dangling and unreacted thiol moieties on the surface of the polymer, the authors were able to successfully functionalize the surface of the microstructure with various ligands by means of a thiol-Michael addition reaction. Although other methods have been described for reaching the same goal in TPP [29, 30], this particular strategy has the advantage of avoiding harsh chemical environments, thus positioning itself in a favorable way for the grafting of TPP microstructures with bio-compatible ligands. In another report, TPP is used to fabricate hydrogel microstructures, taking advantage of the efficient photopolymerization between acrylates and thiols [31]. In this case, the acrylate is a derivative of gelatin hydrolysate while the thiol is provided by the use of reduced bovine serum albumin. Besides the importance of this study for the fabrication of biologically viable three-dimensional scaffolds for tissue engineering, the writing speed employed by the authors to perform TPP is noteworthy. By using a water soluble, rationally designed photoinitiator with a large two-photon cross-section, the authors demonstrate fabrication with writing speed as high as 50 mm/s. Lastly, complex microstructures are presented in a recent report, by using TPP in a clever three-step polymerization process [32]. In the first step, a Diels-Alder reaction transforms a liquid resin into a gel. Then, three-dimensional patterns are written within the gel by TPP, using the photopolymerization of a multifunctional thiol with the oxy-norbornene groups present in the gel matrix. The final microstructure is then exposed by means of a reverse Diels-Alder reaction. The use of a reversibly cross-linked polymer network as described in this report eliminates the sedimentation problem experienced in most liquid negative-tone resins and will be advantageous in applications where fabrication of noncontiguous features in three-dimensions are required.

Herein, we address the difference between an acrylic resin and a thiol-acrylic resin through a direct comparison of their performances when used in TPP. By using commercially available materials (monomers and photoinitiator) and excitation provided by a NIR ultrafast oscillator laser, we aim to provide quantitative observations of the differences between these two types of resins under the most common TPP experimental conditions. Furthermore, we are interested in elucidating the specific advantages and disadvantages in using thiol-acrylic resins for TPP, by investigating writing conditions, writing accuracy, degree of material conversion, and mechanical properties in a comparative manner.

2. Materials and methods

Resins employed in this work consist of a multifunctional acrylic monomer (di-trimethylolpropane tetraacrylate, Sartomer), a multifunctional thiol molecule (pentaerythritol tetrakis (3-mercaptopropionate), Aldrich), and an α-amino ketone photoinitiator (2-benzyl-2-(dimethylamino)-4'-morpholinobutyrophenone, Aldrich). The photoinitiator has maximum linear absorption around 330 nm and it has been shown to be an efficient radical generator for TPP in the emission range of ultrafast NIR lasers [33]. All materials are used as received without any further purification. The acrylic based resin (Acry) is composed of, by weight, 1% photoinitiator and 99% acrylic monomer. Acrylic-thiol resins (AcryS) are prepared by mixing the thiol and acrylate molecules in various concentration ratios. Specifically, AcryS resins with multifunctional thiol concentration ranging from 1.5% to 40% by weight are used. All AcryS resins contain 1% by weight of the photoinitiator. Prior to use, all resins are stirred for 24 hours at room temperature until a homogenous solution is obtained. The resulting viscous liquids are then applied onto microscope cover-slips by drop casting. TPP is started at the resin/substrate interface to ensure that microstructures do not move during the writing process and above all that they may survive the subsequent developing step. After completion of the writing process, the unsolidified part of the resin is washed away in a bath of ethanol, revealing the desired microstructures on the glass substrate. AcryS resins with concentration

#263617 Received 22 Apr 2016; accepted 24 May 2016; published 10 Jun 2016

of the multifunctional thiol molecule higher than 40% led to the instantaneous gelation of the material at room temperature. Therefore, they are not considered in this study.

TPP is performed using a 3D laser lithography system (Photonic Professional, Nanoscribe GmbH) where complex microstructures are formed by either moving the sample around a fixed laser beam or by scanning the laser beam in a fixed sample. Excitation is provided by an ultrafast laser with center wavelength, pulse width, and repetition rate of 780 nm, 100 fs, and 80 MHz, respectively. During microfabrication the laser beam is focused in the resin by means of an oil-immersion objective lens (63x, 1.4NA). Laser average powers reported in this study are all measured before the microscope objective. Imaging of the microstructures fabricated by TPP is performed with a field emission SEM (S4700, Hitachi); prior to imaging all polymeric microstructures are coated with a 5 nm thick layer of chromium.

Two types of microscopies are employed in this study for characterizing microstructures fabricated by TPP. In the first method, information on the polymers degree of conversion is attained using Raman microspectroscopy (InVia H18415, Renishaw) [34]. The excitation source is provided by a 785 nm solid-state diode laser and it is focused into the sample with a 100x objective lens (0.85NA). The same objective lens is used in epi configuration to collect the signal. Raman spectra are recorded with an acquisition time of 10 seconds and with a laser average power of 10 mW. In the second method, a laser scanning microscope is used to collect two-photon induced fluorescence images (BX61, Olympus) [35]. TPP microstructures are excited with 800 nm from a Ti:sapphire oscillator using a 25X microscope objective (1.05NA). Images are constructed using fluorescent signal collected by the same microscope objective; only the signal going through a 40 nm bandpass filter centered at 520 nm is employed.

The mechanical properties of TPP microstructures are accessed with a nanoindenter (TI750Ubi, Hysitron). Indentation is executed with a conical-shape probe having a tip radius of 3 μm. Working times for tip loading and unloading are 20 seconds, while maximum load of 12 mN is held for only 5 seconds to minimize creep behaviors. Microstructures are tested with multiple indentations with depths from 500 nm to 1500 nm to ensure reliable results unaffected by surface roughness and defects.

3. Results and discussions

3.1. Writing conditions

When performing TPP, it is important to constraint laser excitation between the polymerization and damage threshold intensities. If the laser intensity is lower than the polymerization threshold, no sustaining polymerization is induced. If the laser intensity is higher than the damage threshold, the resin boils rendering microfabrication uncontrollable. From a practical standpoint, the polymerization threshold is the minimum value of laser intensity capable of creating polymer features that survive unaltered the developing step. It is desirable for a resin to possess a large writing dynamic range. In this way, voxels with varied dimensions are accessible for optimal realization of microstructures.

To test whether or not the presence of thiol molecules in TPP resins affect the writing dynamic range, we fabricate a three-dimensional microstructure under different experimental conditions using first the Acry resin and then the AcryS resin with 30% by weight of the multifunctional thiol molecule. The microstructure consists of a woodpile geometry with line-to-line and layer-to-layer distances of 2.5 μm and 0.8 μm, respectively. The overall size of the woodpile is 22 x 22 x 20 μm^3. TPP is performed using laser average powers from 15 mW to 60 mW, while writing velocities ranged from 2 mm/s to 5 mm/s. SEM images of arrays of these microstructures are shown in Fig. 1. To help visualize the dynamic range for each resin, microstructures developed with no obvious deformations are highlighted in green. The difference is striking; the window of useful writing parameters for TPP is wider in the case of acrylic based resins when mixed with thiols. For example, at the lowest writing speed of 2 mm/s, TPP is successfully performed in the AcryS resin with laser average powers from 20 mW of 40 mW. Instead, with the Acry resin, only one laser average power (40 mW) results

#263617 Received 22 Apr 2016; accepted 24 May 2016; published 10 Jun 2016

acceptable for performing TPP. As described in the introduction, the multifunctional thiol used in AcryS limits the inhibiting effect of molecular oxygen dissolved in the resin. The laser intensity required to generate the critical amount of radicals for a sustainable TPP is then higher in pure acrylic resins than in acrylates/thiols mixtures. Thus, the overall effect is to expand the writing dynamic range by effectively lower the laser intensity threshold for polymerization.

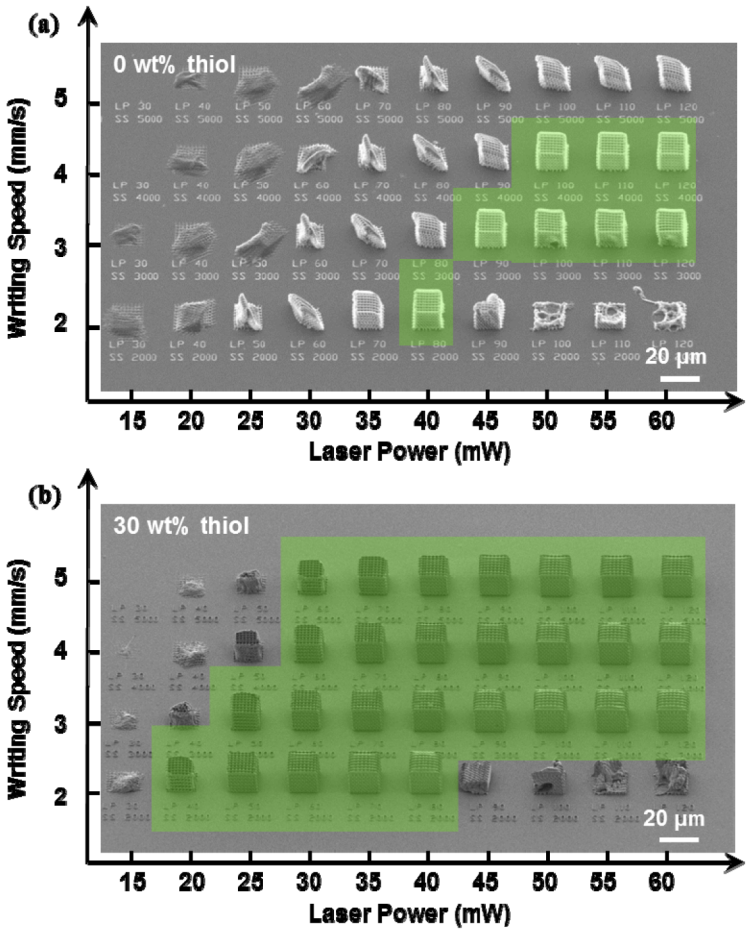

Fig. 1. SEM images of arrays of woodpile microstructures fabricated by TPP using different writing conditions. Resins Acry and AcryS are used in (a) and (b), respectively. Microstructures that survived the fabrication process unaltered are highlighted in green.

Besides expanding the dynamic range of TPP writing, lower laser intensity thresholds induce also the formation of finer voxels. In the next experiment we determine how higher and higher thiol concentrations in AcryS resins influence the polymerization threshold and, consequentially, the size of the formed voxels. To determine these parameters, parallel lines each fabricated using only one laser pass are written across two large supports that are anchored to the substrate. The suspended lines are made with a writing velocity of 20 µm/s, while the laser average power is varied so to have each line produced with a different energy dose. The polymerization threshold is defined in this test as the minimum laser average power capable of creating a stable polymer line which survives the developing step. This line is also used to measure the minimum feature size (i.e. the linewidth). The test microstructures for extrapolating polymerization thresholds and corresponding linewidths are fabricated using the

#263617 Received 22 Apr 2016; accepted 24 May 2016; published 10 Jun 2016

Acry and AcryS resins with multifunctional thiol molecule concentrations ranging, in weight percent, from 10 to 40.

The results are plotted in Fig. 2(a). The polymerization threshold for the Acry resin is 6 mW. By adding larger and larger amounts of the multifunctional thiol molecule in the resin mixture, a monotonic decline in the measured polymerization threshold is observed reaching a value of 2 mW for thiol concentration larger than 30% in weight. The corresponding linewidths of the features created at polymerization thresholds (i.e. minimum feature size) follow a slightly different trend. First, the smallest achievable linewidth for the Acry resin is about 290 nm (Fig. 2(b)). Then, it gradually diminishes as more and more multifunctional thiol molecule is added into the AcryS resins. The smallest linewidth of 183 nm is measured in the resin with 30% in weight of multifunctional thiol molecule (Fig. 2(b)). Finally, the trend is reversed, and a dramatic increase in the linewidth is measured in the resin with 40% in weight of the multifunctional thiol molecule with a value of 439 nm.

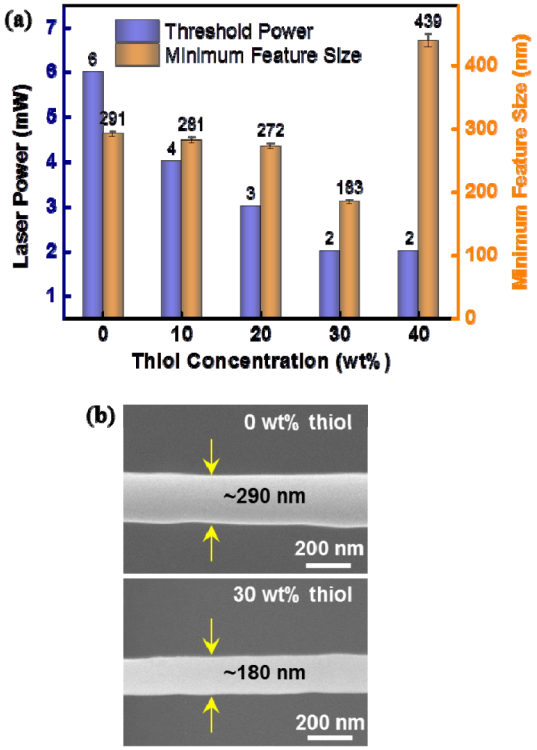

Fig. 2. (a) Dependence of polymerization thresholds and minimum feature size on thiol concentration used in TPP resins. While polymerization thresholds decrease with increasing thiol concentration, the smallest linewidth is obtained at a thiol concentration of 30% by weight. (b) SEM images of suspended lines fabricated with the Acry resin and with the AcryS resin containing 30% by weight of the multifunctional thiol molecule.

There are two competing mechanisms in the fabrication of these microstructures when using AcryS resins. Depending on the concentration of the multifunctional thiol molecule, one must play a stronger role than the other one. For thiol concentration up to 30% in weight, the depression of the polymerization threshold allows using lower laser average powers and thus creating smaller feature sizes. When the thiol concentration exceeds 30% in weight, the resin gelation time is delayed with the effect of creating favorable conditions for radicals' diffusion. Furthermore, an increase in thiol concentration translates also in an increase in thyil radicals in the late stage of the polymer formation favoring what is known as the "dark reaction" [36]. Both of these phenomena are plausible explanations for the observed increase

#263617 Received 22 Apr 2016; accepted 24 May 2016; published 10 Jun 2016

in the minimum feature size in AcryS resins with thiol concertation larger than 40% in weight.

It is well-known that at even low concentrations, thiols molecules are capable of accelerating the polymerization rate of several kinds of olefins [26]. In the case of (meth)acrylates, reduction of conversion times by an order of magnitude have been reported [27]. This aspect of thiol-ene networks photochemistry is particularly useful in applications where the photoinitiator concentration needs to be minimized, such as the fabrication of biocompatible structures and the curing of highly pigmented films. Enhancement of the polymerization rate is important in TPP also. Indeed, parts production in TPP is a serial process. Thus, any strategy that allows for writing microstructures faster is an important advancement in the field. Among the several physical and chemical methods used so far to increase writing speed in TPP, the development of efficient photoinitiators with large two-photon cross-sections is certainly the method that has produced the most outstanding results [37].

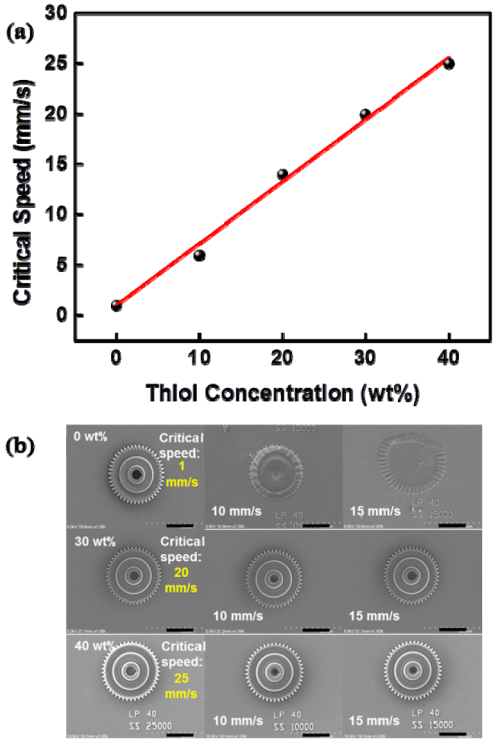

Fig. 3. (a) TPP writing critical speed dependence on the concentration of multifunctional thiol molecule used in resins. The red line is a linear regression. (b) SEM images of representative micro-gear structures used to extrapolate critical speeds for three of five resins used in this study (scale bars 20 μm). The images in each row represent microstructures fabricated out of the same material but with different writing speeds. The weight percentages on the top left images are the concentrations of the multifunctional thiol molecule used in the three resins (see Visualization 1).

To determine the effect of thiols concentration on the writing speed when performing TPP, we measure the critical speed for five different resins. The critical speed is defined as the maximum speed at which fabrication of a microstructure occurs without the presence of mistakes (either during the writing or the developing step). A micro-gear is chosen as the test design because of the complexity of its topology. At a fixed laser average power of 20 mW, a series of micro-gears are fabricated using faster and faster writing speeds.

#263617 Received 22 Apr 2016; accepted 24 May 2016; published 10 Jun 2016

The test is repeated with resin Acry and resins AcryS with a multifunctional thiol molecule concentrations ranging from 10% to 40% in weight. Each measurement is repeated at least three times to ensure repeatability. The results are plotted in Fig. 3(a), where a remarkable increase in TPP writing speed is observed. As the concentration of thiol molecules in the AcryS resin increases, a consistent increase in the critical speed id observed too. The presence of 40% by weight of the multifunctional thiol molecule in the acrylic resin is capable to boost the critical speed from 1 mm/s to 25 mm/s. Representative SEM images of the micro-gears used in the critical speed test are shown in Fig. 3(b) for three of the resins. The failed microstructures obtained when using writing speeds higher than the critical speed are shown for the Acry resin where, at speed of 10 mm/s and 15 mm/s, incomplete and deformed micro-gears are formed. A video illustrating the difference between TPP writing speeds in Acry and AcryS resins is provided in the Supplementary Information.

3.2. Physical and mechanical properties

The mechanical properties of polymers generated by the photopolymerization of thiol-ene mixtures have been studied extensively [38]. Since these resins can produce highly uniform crosslinked networks with reduced internal stresses and reduced overall shrinkage, they have found applications in the formation of high-energy absorbing materials and in the UV curing of thin films [39]. In these cases, photopolymerization is typically carried up with a flood light illumination. Although microfabrication by TPP is performed using a diametrically opposite excitation procedure (point-by-point), one will still expect to see some benefits in the physical and mechanical properties of TPP microstructures when using thiol-ene mixtures.

To explore whether or not this assumption is correct, we study the difference in the material stiffness between TPP microstructures created with the Acry resin and with the AcryS resin containing, in weight, 30% of the multifunctional thiol molecule. Five suspended bridges with different lengths ranging from 40 μm to 120 μm are fabricated by TPP in each resin. The polymeric bridges are formed using multiple laser passes with line-to-line and layer-to-layer separations of 200 nm, resulting in a 5 x 2 μm^2 cross section. Writing conditions for microfabrication are 25 mW and 5 mm/s for the laser average power and writing speed, respectively. SEM images of these microstructures are shown in Fig. 4(a). With the exception of the two shortest ones, the bridges made from the Acry resin present ample physical deformations. By contrast, all the bridges made from the AcryS resin survived unaltered the developing step.

Encouraged by the qualitative results obtained in the previous test, we embark in a more systematic study of the mechanical properties of TPP microstructures using this time nanoindentation. The sample employed in this set of measurements consists of a solid polymeric box 20 μm long, 20 μm wide and 10 μm tall. With equal writing conditions (laser average power of 25 mW and writing speed of 100 μm/s), the test samples are fabricated by TPP using a series of resins from Acry to AcryS with varied concentrations of the multifunctional thiol molecule. The results of the nanoindentation measurements are shown in Fig. 4(b), where the reduced Young's modulus (E_r) and hardness (H) of the TPP microstructures are plotted versus the concentration of thiol in the resins. Both E_r and H increase steadily with increasing thiol concentration with a maximum effect achieved in the AcryS resin containing, in weight, 30% of the multifunctional thiol molecule. In this range, E_r and H experience a 2.6- and 3-fold enhancement, respectively. However, this trend is reversed almost completely when the thiol concentration in the AcryS resin becomes larger than 30%, with E_r and H plunging to values similar to the ones measured for the Acry resin.

From the results collectively shown in Fig. 4, it is evident that microstructures prepared using resins based on acrylate-thiol mixtures are stronger than microstructures prepared using pure acrylic resins. Therefore, TPP applications that require the construction of rigid architectures will benefit by using AcryS resins. The results from Fig. 4 point out also to the fact that an excessive amount of multifunctional thiol molecules in the AcryS resins has the opposite effect on the mechanical properties of TPP microstructures, and that is to make them softer. This outcome, which is observed also in polymers generated by the UV curing of the

#263617 Received 22 Apr 2016; accepted 24 May 2016; published 10 Jun 2016

same resins, stems from two characteristics of thiol-ene mixtures polymerization [40]. The first characteristic is the generation of a larger number of polymer chains with reduced average molecular weights as the concentration of thiol molecules increases in the resin. The second characteristic is the strengths of the atomic bonds found within the final polymer network. Since the energy of the C-S bond is lower (272 kJ/mol) than the energy of the C-C bond (346 kJ/mol), increasing the concentration of thiol molecules in the AcryS resins has the net effect of producing polymer with larger concentration of C-S bonds, thus creating weaker and more flexible polymers.

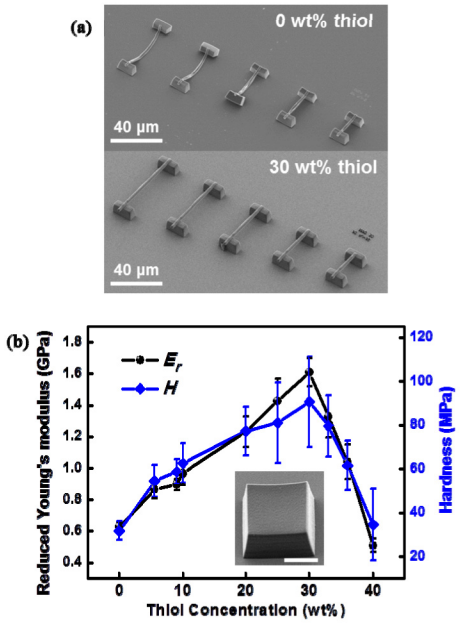

Fig. 4. (a) SEM of micro bridges fabricated by TPP using the Acry resin (top image) and the AcryS resin (bottom image) containing 30% in weight of the multifunctional thiol molecule. (b) Reduced Young's modulus (Er) and Hardness (H) values retrieved from TPP microstructures built from resins containing varied concentration of the multifunctional thiol molecule. SEM of the test microstructure used in the nanoindentation measurements is shown in the figure's inset (scale bar 10 µm).

While multifunctional acrylates are commonly used in TPP resins because they produce highly cross-linked and thus rigid polymer networks, their polymerization is accompanied by a considerable amount of shrinkage. This phenomenon is quite adverse when high fidelity in the reproduction of a complex structure is required, since it produces undesirable distortions. Several strategies have been implemented in TPP to overcome this drawback. They include structure design precompensation, implementing solid support frames, and using sol-gel organic-inorganic hybrid technology for developing novel resins [16,41,42]. The latter method is the easiest to implement and delivers the most consistent results. One strategy not yet investigated for reducing polymerization shrinkage in TPP is the use of thiol-ene chemistry.

It has been shown that the polymerization of (meth)acrylates by UV curing proceeds with limited shrinkage when thiol molecules are added to the resin mixture [25]. The shrinkage associated with the polymerization of (meth)acrylates is 22-23 cm^3/mol per reacted double bonds, while it is between 12 and 15 cm^3/mol in the case of thiol-(meth)acrylate polymerization [43]. To confirm this improvement imparted by the use of thiol molecule in (meth)acrylate resins in TPP also, we fabricate a series of microstructures with resins containing different amount of the multifunctional thiol molecule. The test structure consists of a 16-layer woodpile with rod-to-rod and layer-to-layer distances of 2.5 µm and 0.8 µm,

#263617 Received 22 Apr 2016; accepted 24 May 2016; published 10 Jun 2016

respectively. The structures are all made using 8 mW laser average power and 20 μm/s writing speed. The percentage of shrinkage (PS) is extrapolated by measuring the length difference between the top and bottom layers of the woodpile structure. Figure 5 shows that the shrinkage of the Acry resin is around 18%. As the concentration of the multifunctional thiol molecule in the AcryS resins reaches 10% in weight, the shrinkage of the microstructure drops of more than half from its original value to around 6%. A further increase in the thiol concentration produces only a minor improvement, with shrinkage approaching 4% at a multifunction thiol molecule concentration of 40% by weight.

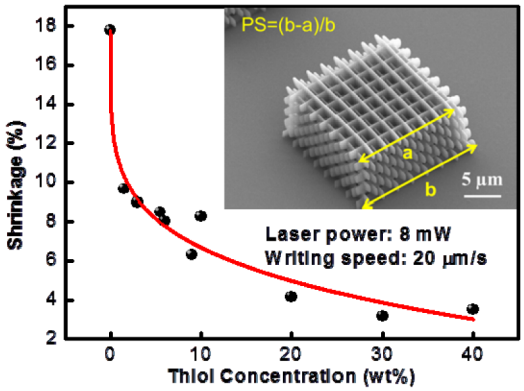

Fig. 5. Shrinkage of a woodpile microstructure fabricated by TPP using acrylic resins with different concentrations of multifunctional thiol molecule. The data is fitted to an exponential decay (red line) to guide the eye. A SEM image of the test microstructure with the definition of percentage of shrinkage (PS) used in this study is shown in the inset.

3.3. Raman and fluorescence characterization

In the previous two sections, we highlighted the fabrication improvements achieved when a multifunctional thiol molecule is added to a standard acrylic-based resin employed in TPP. These improvements are a direct consequence of the chemistry involved in the thiol-acrylate polymerization. Specifically, cross-linked networks are rapidly generated with an onset of the gel state that occurs only at high degree of monomers conversion. Therefore, thiol-acrylate resins produce polymer with a more uniform distribution of cross-linking and with larger degree of conversions than their pure acrylate counterparts. Several reports have shown the usefulness of Raman microspectroscopy in characterizing the chemical changes occurring in resins during TPP [33,34,44]. Here, we exploit the same technique to evaluate the degree of conversion obtained with Acry and AcryS resins.

The samples for Raman characterization include a series of solid boxes with dimensions of 20 μm x 20 μm x 10 μm fabricated by TPP using 10 mW of laser average power and a writing speed of 20 μm/s. Measurements are performed on samples made from the Acry resin and from AcryS resins containing a concentration in weight of the multifunctional thiol molecule from 1% to 40%. The radial and axial hatching spacing implemented in the formation of each box are chosen accordingly to obtain the same filling ratio in all microstructures. Raman spectra of TPP microstructures produced under these conditions from the Acry resin and from AcryS resins containing 10%, 20%, 30%, and 40% in weight of the multifunctional molecule are plotted in Fig. 6(a). We focus our attention in the spectral region between 1550 cm^{-1} and 1800 cm^{-1}. In this section of the fingerprint region, three distinct Raman peaks are presents that are useful in understanding the polymerization chemistry of the resins involved in this study. The peaks at 1630 cm^{-1} and 1720 cm^{-1} are ascribed to the vibrational modes of the olefin and carbonyl moieties, respectively. While the first one derives exclusively from the multifunctional acrylate, the second peak receives contributions from the vibrations of the carbonyl groups present in the acrylic monomer and the thiol

#263617 Received 22 Apr 2016; accepted 24 May 2016; published 10 Jun 2016

molecule. Since both resin components have the same functionality (4), the number of carbonyl groups present in any of the Acry or AcryS resins remains always the same, independently of the mixing ratios. The third peak at 1600 cm^{-1} is ascribed to the ring vibration mode of the photoinitiator.

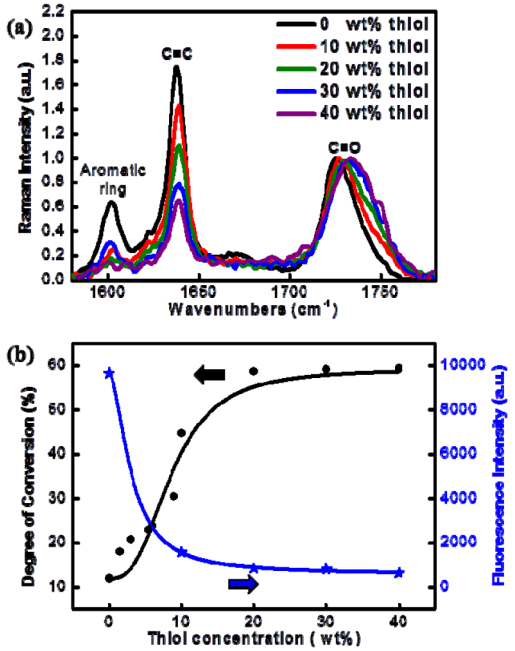

Fig. 6. Raman spectra of TPP microstructures fabricated using the Acry resin and AcryS resins with different concentrations of the multifunctional thiol molecule. Each peak is label with the chemical moiety responsible for that vibration mode. (b) Degree of conversion (left) and fluorescence (right) of TPP microstructures as a function of thiol concentration. The black and blue lines are drawn only to guide the eye.

The carbonyl groups in either the acrylate monomer or the thiol molecule do not participate in the polymerization reaction and, consequentially, their number remains the same. This observation is confirmed in Fig. 6(a) where the spectra of five polymers show intensities for their corresponding 1720 cm^{-1} peak that are almost identical with each other (the small variations measured in the peak position are most certainly due to variations in the local chemical environments). During radical polymerization of acrylic monomers, carbon/carbon double bonds are consumed over time creating carbon/carbon single bonds. It is through these newly formed bonds among monomers that the polymer is formed. The spectra in Fig. 6(a) show a clear contraction in the intensity of the peak related to the monomer carbon/carbon double bond with the increase of the thiol concentration. Although part of this trend is due simply to a lower concentration of the acrylic monomer in the initial resin, the magnitude of the carbon/carbon double bond signal decline in Fig. 6(a) can be explained only by taking into consideration the role of the multifunctional thiol molecule in the resin polymerization. Because of the generation of thyil radicals, the polymerization of thiol-acrylate resins proceeds with overall larger monomers conversion than the polymerization of acrylate resins. Thus, we expect a lower and lower intensity for the 1630 cm^{-1} peak as the concentration of thiol increases.

To quantify this observation, we measure the polymer degree of conversion (DC) as it occurs during TPP for the Acry and the AcryS resins in function of thiol concentration. A detail description of the methodology employed to extrapolate DC values from TPP microstructures' Raman spectra can be found elsewhere. Briefly, for each mixture, the Raman spectra of the unpolymerized and polymerized resins are collected using the same excitation

#263617 Received 22 Apr 2016; accepted 24 May 2016; published 10 Jun 2016

and collection conditions. For the polymerized resin, TPP microstructures as the ones used for producing the graphs in Fig. 6(a) are employed. DCs are calculated using the integrated intensities of the olefin and the carbonyl peaks measured for the resins and the polymers. Since the number of carbonyl groups in the resins remain the same during polymerization, the peak at 1720 $cm^{-1}$is used as an internal reference. The decrease in the number of carbon/carbon double bonds in the resins mixed with the multifunctional thiol molecule is accounted for in the DC findings. The results are shown in Fig. 6(b). Under the writing conditions employed for TPP (10 mW, 10 µm/s), the Acry resin has a DC that is barely over 10%. Instead, with the same TPP writing conditions, the AcryS resins acquire DCs that grow rapidly with the increase of thiol concentration in the resin. Only 10% in weight of the multifunctional thiol molecule produces a polymer DC of 30%. A plateau of the DC at around 60% is observed for thiol concentrations larger than 20% in weight. This outstanding augmentation of polymer DC is accredited to the combination of step-growth and chain growth processes that develops in the TPP of thiol-acrylate resins.

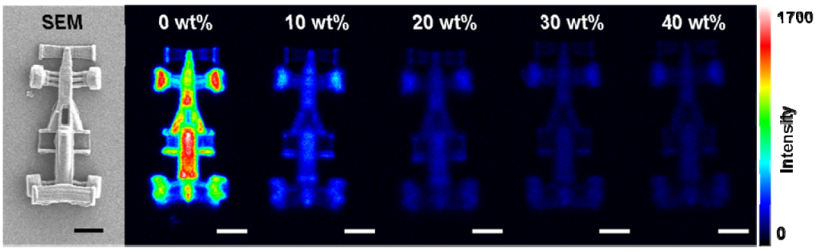

Fig. 7. SEM and TPM images of micro-cars fabricated by TPP (LUT shown in far right). The numbers in the fluorescence images reflect the thiol concentration in the Acry and AcryS resins employed for this experiment (scale bars: 10 µm).

While acquiring the data for the aforementioned study, we notice that the Raman background signal tend to diminish with increasing concentration of the multifunctional thiol molecule. Since the nature of this background signal is polymer autofluorescence, we characterize it by means of two-photon induced fluorescence microscopy, in brief two-photon microscopy (TPM). We first fabricate by TPP a series of test structures from the Acry resin and from AcryS resins with thiol concentration by weight of 10%, 20%, 30%, and 40%. All the microstructures are produced with identical writing conditions. Then, fluorescence cross-sections of these microstructures are recorded by TPM. Figure 7 displays the SEM of the test sample; it consists of the reproduction of a Formula 1 car having tires no more than 2 µm wide. Furthermore, fluorescence cross-sections of the TPP microstructures created from the different resins are shown in Fig. 7. As the LUT on the right of this Figure shows, the fluorescence signal decrease substantially as the thiol concentration increases. To quantify this effect, the integrated fluorescence intensity (in relation to the images in Fig. 7) is plotted in function of the resin thiol concentrations in Fig. 6(b). Fluorescence from TPP microstructures follows an evolution with increasing thiol concentration that is diametrically opposite to the one measured for the microstructures DC. While fluorescence signal is the largest for the Acry resin, it decreases rapidly for AcryS resins reaching a minimum when the thiol concentration by weight is 20%.

Because of the long excitation wavelengths and the relative low intensities used for excitation, the most probable cause for the polymer autofluorescence is the photoinitiator. Subsequent to light absorption, the photoinitiator undergoes a homolytic cleavage forming two reactive radicals that start the polymerization process. Therefore, the photoinitiator is consumed during radical photopolymerization. This aspect of the resins polymerization is visible in the Raman spectra of Fig. 6(a). The polymers with larger concentration of the multifunctional thiol molecule present the smallest signals for the 1600 cm^{-1} peak. Since the vibrational mode that generates this peak is characteristic of the photoinitiator only, this data suggests that photoinitiator concentration is depleted in a larger extend in the AcryS resins

#263617 Received 22 Apr 2016; accepted 24 May 2016; published 10 Jun 2016

than in the Acry resin during TPP. Hence, the fluorescence trend observed in the polymeric microstructure and plotted in Fig. 6(b).

4. Conclusion

We have investigated the use of thiol-acrylate resins in TPP. Because of the numerous advantages the thiol-ene chemistry impart to the mechanism and the results of photopolymerization, we have studied in a comparative way the difference between a pure acrylic resin and a series of resins with varied amounts of a multifunctional thiol molecule. Many TPP performances are improved when thiol-acrylate resins are used. In particular, we measure stronger polymers, and we observe better writing conditions such as a wider dynamic range for usable laser average powers and larger fabrication speeds. Finally, polymer DCs are measured by Raman microspectrometry proving that the improvement of the mechanical properties of TPP microstructures when using thiol-acrylate resins is due to larger monomer conversion.

Aknowledgments

This research work was financially supported by the National Science Foundation division of Civil, Mechanical and Manufacturing innovation (CMMI 1068510 and 1129613) and the Nebraska Center for Energy Research (NCESR). Lijia Jiang and Wei Xiong contributed equally to this work.

#263617 Received 22 Apr 2016; accepted 24 May 2016; published 10 Jun 2016